Preparation and Performance Research of Baking-Carbonized Functional Flavors/Konjac Glucomannan Porous Composite Membrane

doi: https://doi.org/10.3233/ATDE220818

Proceedings of the 2022 International Conference on Smart Manufacturing and Material Processing (SMMP2022), A. Nayyar (Ed.)

doi:10.3233/ATDE220818

Preparation and Performance Research of Baking-Carbonized Functional Flavors/Konjac Glucomannan Porous Composite Membrane

Ling ZHANG [a], Jinkun LIU [b], Yanqing DUAN [a], Wei ZHE [a], Yingliang ZHAO [a], Toshiki Miyazaki [c] and Chao LI [a,1]

[a] *R&D Department II, R&D Center of China Tobacco Yunnan Industrial Co., Ltd., Kunming, 650231, China*

[b] *Faculty of Materials Science and Technology, Kunming University of Science and Technology, Kunming, 650093, China*

[c] *Graduate School of Life Science and Systems Engineering, Kyushu Institute of Technology, Japan*

Abstract. To develop one porous additive material that can be assembled on cigarette filter, and achieve both functions of reducing hazard substances like tar and providing special aroma and moisture, this study innovatively selects the raw materials like baking-carbonized functional flavors with special aroma and konjac glucomannan (KGM) with properties of water absorption, gelling and film-forming, following the steps of casting into membrane shape, thermostatic crosslinking for strength enhancement and freeze-drying for pore creating to prepare 5 porous composite membranes based on baked-carbonized functional flavors and konjac glucomannan (KGM) were prepared. The composite structure, morphologies on the surface and the cross section, porosity structures including mesoporous and macropore of the porous composite membranes were characterized, the tensile performance and aroma constituents through solid phase microextraction and hazardous substances adsorption as packed into the commercial cigarette were also studied. Results showed that all baked-carbonized functional flavors were carbonized into amorphous, and contained the groups of aromatic components like ≡C-H, C=O, C-O-C (aldehydes, esters), cross-linking achieved the entanglement of KGM segments by deacetylation. When compounded, KGM acted as the framework to build the 3D porous network structure, and the functional flavor powders were wrapped into the KGM layer. All porous composite membranes owned some mechanical strength and the internal porosity over 90%, the mesopores and the macropores were ranged with 5-50nm and 20-255μm, respectively, which was satisfied for gas flowing and harmful substances adsorption. Aroma and resulting abundance of extracted constituents changed with timing, which equipped the membranes with a comprehensive aroma feeling. Among them, the membrane prepared with the raw material of dark plum showed a better comprehensive performance, especially it could significantly reduce the contents of harmful HCN and phenol in cigarette during smoking.

Keywords. Konjac glucomannan, baking-carbonized flavors, porous composite membrane, porosity structures, aroma-constituents evaluation, harmful components reduction

[1] Corresponding Author: Chao Li, 403293417@qq.com.

1. Introduction

Facing the health issues brought by smoking, low-harm cigarettes have become the first choice for the consumers, and an inevitable trend for the tobacco industry. In current research and development about the low-harm cigarettes, the purpose of achieving tar and other harms reduction is popular with the methods such as blending expanded cut tobacco and expanded cut stems, perforating the filter rod for ventilation and dilution or adding adsorbent materials into the filter rod [1,2], but the practice application has proved adding adsorbent materials into the filter rod is more effective. Available adsorption materials included the activated carbon, sepiolite, zeolite, silica gel, molecular sieve and so on [3-5]. Although they have been reported with good adsorption effect on harm substances, they also bring negative impacts like attenuating the smoking taste even introducing other bad smells, which turns the adsorption materials have to be replaced with more advanced new ones. In addition, the commercial cigarettes also face another drawback that the smoke taste is relatively simple and lacks of rich hierarchy sense, owing to the flavor constituents mainly come from the tobacco leaf itself [6]. While to the artificial flavors on market, liquid lipids or tinctures are not suitable for cigarettes, the aromas of solid flavors are hard to blend with that of tobacco, and harmful gas emitting on combustion make some of them be abandoned [7,8]. Now the studies on smoke taste enhancement are focusing on the natural plants with environment-friendly, especially more aromas about them can be further stimulated out after being treated with baking, carbonization and fermentation, but unfortunately, the adsorption capacities of these carbonized flavors are still weak [9,10]. Therefore, seeking other absorbent materials to make the composite is necessary to realize both actions of absorbing harmful constituents and enhancing aroma emitting, which is also a hot issue to be solved urgently in the development of low-hazard cigarettes.

Considering the pore advantages from traditional absorbent materials, and the doubt that loading additional substances leads to lower the intrinsic adsorption capacity [11,12], the ideal candidates should build a three-dimensional porous network in structure including the mesopores and the macropores, and its expandable volume combined with the processing technology is able to swallow these flavor powders inside the material itself instead of filling into the pores. Those that can meet mentioned-above conditions only leave to the natural polymers like konjac glucomannan, hyaluronic acid, chitosan, collagen and so on. Among these macromolecules, Konjac glucomannan (KGM) is the extract from the konjac corm under chinese species Araceae, usually owns advantages of wide source, low cost and good safety [13]. In Asia, KGM is listed as dietary fiber, which can help to weight loss, promote intestinal peristalsis and lower blood cholesterol [14]. In the United States, KGM is an FDA-approved emulsified thickener which could be applied in medicines and cosmetics [15,16]. The basic unit of KGM is shown in Figure 1, which contributes to construct the final tertiary structure [17], the first level is a linear one composed of glucose and mannose as repeating units according to a certain molar ratio, the second level is a two-fold helix presented by the extension of KGM main chains, and the third level is the 3D network based on the rotation of the secondary structure. Owing to such unique structure, KGM exhibits physicochemical characteristic summarized as rheology, thickening, gelling, film-forming and water retention property [18-20], especially the gelling and film-forming, which make it possible to process KGM into membrane [21,22].

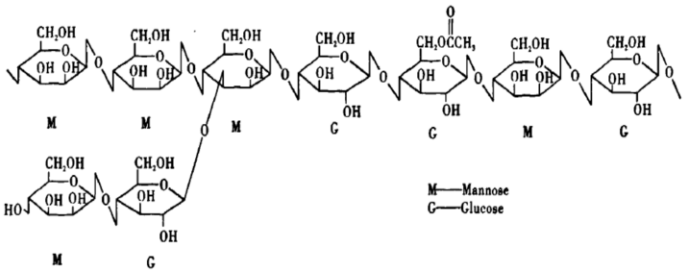

Figure 1. Basic structural unit in konjac glucomannan chains.

Baking-carbonization is processed at a relatively low-temperature, the natural herbaceous plants experienced this treatment changes into carbon materials, meanwhile, it retains the aroma sources from raw materials, which can be realized a certain aroma enhancement effect [23,24]. Freeze-drying technology is a new pore-forming technology which utilizes the lower sublimation point under high vacuum (10-40Pa) to directly convert the moisture inside the material from the solid state to the gaseous one, which makes almost no changes to the chemical composition. Once the freeze-drying is applied to KGM, it is verified to create more pores and higher porosity [25-27].

As concluded to the mentioned characteristics of baking-carbonized flavors and KGM, and the pore-creating advantage of freeze-drying, the composite membranes based on both raw materials were produced following the processes of the tape casting, crosslinking and freeze drying, the structure, internal sectional morphology and pore information of the porous composite membranes are investigated, which is expected to ensure that the flavor continuously emits the special aroma and the mesoporous pores absorb harmful substances at smoking. And the composite membrane with better overall performance could be further used in the filter rod to improve its function.

2. Materials and methods

2.1. Materials

Food-grade Konjac glucomannan (KGM) powders purchased from Xieli Konjac Scientific Planting & Processing Community Co., Ltd. (Chengdu, China) were passing through 120 mesh sieve in advance. Concentrated ammonia ($NH_3 \cdot H_2O$) was brought from Bodi Chemical Co., Ltd. (Tianjin, China). Natural herbaceous Resources for baking-carbonized products were chosen as the Dark Plum, Rosa Roxburghii Tratt, Pu'er Tea, Phlomis Betonicoides and White Tea, all of these were derived from the local places of Yunnan province in China.

2.2. Preparation

2.2.1 Preparation of baking-carbonized flavors

All mentioned herbaceous resources (Dark plum, Rosa Roxburghii Tratt, Pu'er tea, Phlomis Betonicoides and White Tea) were heated at 90℃ for 10h to remove residual moisture, further baked into the furnace for deep carbonization under an air-isolated environment, the carbonization temperature and time were listed in Table 1. The carbonized resources were sprayed with the Bacillus Subtilis of *Van3*, then fermented

at 22℃ for 24h under the relative humidity over 60%. After being grinded and crushed, all products passing through 200 mesh in powder were obtained as the baking-carbonized functional flavors.

Table 1. Preparation parameters of baking-carbonized flavors under different resources.

Sample Naming	Herbaceous Resource	Carbonization Temperature (ºC)	Baking time (h)
ZYFJ (TH)	Dark Plum	200	16
ZYFJ	Rosa Roxburghii Tratt	180	10
NTHPEC	Pu'er Tea	160	15
NTHXGXG	Phlomis Betonicoides	250	20
WBTM	White Tea	150	12

2.2.2 Preparation of porous composite membrane

The porous composite membrane was proceeded with following steps: 1g KGM and 1g baking-carbonized functional flavor were added into 50ml of deionized water and stirred until all of them were well-mixed, then the mixture was microwave-assisting heated at 350W for about 1.5 minutes, and then defoamed under negative-pressure filtration. After that, a certain amount of concentrated ammonia as the cross-linker was added into the mixture by dropwise under continuous stirring. Waiting for turning into the sol state, the mixed sol was casted into a tailor-made mold with the internal size of Φ200 × 1mm2 ± 0.1mm, and immersed into a curing liquid composed of ethanol and glycerol (volume ratio: 4: 1) for demolding. Once being successfully separated off, the membrane type composite was cross-linked at 90.5oC for 8h, pre-frozen at -40oC overnight and then freeze-dried at a vacuum condition until complete dehydration. The baking-carbonized functional flavor/KGM porous composite membranes were finally obtained. In addition, the KGM porous membrane without any flavor as the control was also produced under the same procedure.

2.3. Characterizations and Measurements

2.3.1 Characterizations

Potential phases of baking-carbonized flavors were checked through the X-ray Diffractometer (RIGAKU D/max 2550VB/PC, Japan) recorded patterns under the scanning step of 2°/min, their containing functional groups were monitored by Fourier Transform Infrared (FT-IR) spectrometer (THERMO FISHER Nicolet iS10, USA) with the wavenumber ranged from 400cm-1 to 4000cm-1. Surface and internal cross-section morphologies were investigated through the Scanning Electron Microscope (SEM, TESCAN MIRA4, Czech Republic), and the resulting mesoporous and macroporous information was acquired from the Automated Surface Area and Porosity Analyzer (BET, MICROMERITICS ASAP2460, USA) and the Automatic Mercury Porosimeter (QUANTACHROME PoreMaster GT 33/60, USA), respectively.

2.3.2 Tensile properties Testing

Tensile properties of the baking-carbonized functional flavor/KGM porous composite membrane were tested on a universal testing machine (HENGYI Instrument HENGYI-2550, China), which required the membrane sample to be cut into a beam shape of 50 × 10 × 1mm3 ± 0.1mm, the holder to be applied to make the clamping distance at 30mm, and the loading displacement was set as 1mm/min. In testing, the sample turned to be broken under tensile move, the strength at break was defined as the tensile strength, and the elastic modulus was calculated based on the linear interval of the stress-strain

curve. Each membrane needed 5 repetition tests, both strength and modulus were expressed as the mean ± sd.

2.3.3 Extract ingredients measurements

Gas chromatography-mass spectrometry (GC/MS, Bruker SCION TQ GC-MS/MS, USA) was used to detect and analyze the components in the porous composite membrane. Specifically, 0.2g of the sample was taken into a headspace vial, and dichloromethane was used as a solvent for extraction in a solid-phase microextraction cabin at 80°C and 250r/min for 30min, and the desorption time was 3min. The analysis conditions were set as follows: He gas player as the carrier flow, the inlet temperature, the flow rate and the split ratio were set as 240°C, 1.5mL/min in constant flow mode and 10: 1, respectively. DB–5MS column (60m×0.25mm i.d.×0.25μm d.f.) were chosen, and the ionization energy was maintained at 70eV; the solvent delay time was 1.5min. NIST spectral library was used to search, and the method was full scan monitoring mode with the scanning range of 40-500amu.

2.3.4 Hazardous substances contents determination

Optimal porous membrane was cut into the piece with surface size of 2 × 2mm2, then packaged into the filter of the commercial cigarettes called Yunyan. After being lighted, 7 Hazardous substances in the smoking would be tested, and the normal Yunyan cigarette was chosen as the control.

3. Results and Discussions

3.1. Characterizations on baking-carbonized flavors and KGM

Figure 2 is the XRD diffraction patterns of the baking-carbonized functional flavors prepared by the herbaceous resources. It was seen that there was only one broad diffraction centered at about 22° to each sample, since it was defined as the typical peak that represented amorphous, combining with the carbonization treatment to all resources, it could be confirmed that all flavors were amorphous carbon material. In addition, there was no significant difference on XRD patterns, it meant the carbonization at relatively low temperature had not changed the basic ingredients in original herbaceous resources, more details needed to be further explored by FT-IR.

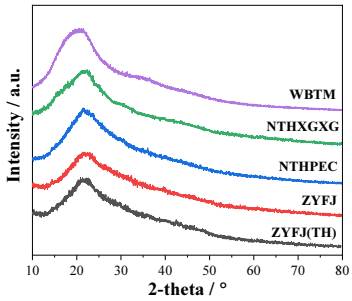

Figure 2. XRD patterns of baking-carbonized functional flavors.

Since the residual ingredients are more complicated, the survey on them was carried out in terms of the contained groups in baking-carbonized functional powders, and the FT-IR spectra was shown in Figure 3(a). The wavenumber indicated that the

infrared absorption peak at 3417cm^{-1} was corresponding to the vibration of OH^- group, the peak at 3230cm^{-1} was the hydrocarbon ≡C-H stretching, the peaks at 2962cm^{-1}, 2925cm^{-1}, 2859cm^{-1} belonged to the ≡C-H stretching, and the ones at 2859cm^{-1}, 1645cm^{-1}, 1616cm^{-1}, 1401cm^{-1}, 1322cm^{-1} and 1242cm^{-1} were attributed to the groups of CH_2, C=O (lipid, aldehyde, ketone, acid), C=C, COO-, CH_2 and C-N, respectively. Other groups like C-O-C from aldehyde) C-O-C from ester, -OCH_3, CH_2 were located at the wavenumber of 1159cm^{-1}, 1105cm^{-1}, 1045cm^{-1} and 780cm^{-1}. Besides that, there was a R-O vibration detected at 595cm^{-1}, and R represented N, P or other elements. All of these functional groups were existed in the flavor samples of ZYFJ (TH), ZYFJ, NTHXGXG and WBTM. To NTHPEC, additional groups such as =C-H, C=O, C-O, and COH from carboxylic acid were also detected, but the antisymmetric stretch of -OCH_3 at 1045cm^{-1} disappeared. The functional groups indicated the aroma of prepared flavors came from aldehydes, ketones, hydrocarbons, lactones, alcohols, acids and esters, which was consistent with our acknowledge about the sources like the ones in perfume.

FT-IR spectra of KGM including the original powder, uncrosslinked and crosslinked membranes is figured in Figure 3(b). Compared KGM powder with uncrosslinked KGM porous membrane, the peaks on infrared spectra were all derived from konjac glucomannan itself and kept almost the same, potentially suggested that physical processing technology like tape casting and freeze-drying would not change the chemical nature of raw material. While to the cross-linked KGM porous membrane, the CH_3-C=O- group at 1732cm^{-1} and the C=O group at 1024cm^{-1} were found to disappear, due to the broken of C=O bond. And the dehydration and condensation made -CH_2OH and -OH on KGM chain to form new unsaturated C-O-C bond, which could be proved the increase in the absorption intensity of the C-O group at 1255cm^{-1}.

Comparing the KGM raw material and the uncrosslinked KGM porous membrane, the infrared spectra are basically the same, and the group structure is all derived from konjac glucomannan itself, potentially indicating that the physical treatment process such as tape casting and freeze-drying will not change the composition of the raw material. In contrast to the cross-linked KGM porous membrane, it was found that the ethanoyl (CH_3-C=O-) group at 1732cm^{-1} and the C=O group at 1024cm^{-1} disappeared, and the dehydration and condensation under crosslinking made -CH_2OH and OH on KGM branched chain to form an unsaturated C-O-C structure, which can be supported by the increase of the peak intensity of C-O group at 1255cm^{-1}. Crosslinking relied on the deacetylation, contributed to increase the entanglement of molecular chains, and further improved the mechanical properties of target materials [28,29].

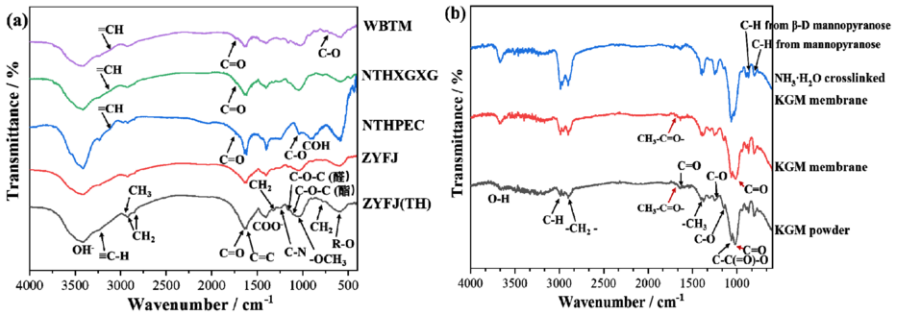

Figure 3. FT-IR spectra of (a) baking-carbonized flavors and (b) KGM powder, its non-crosslinked and crosslinked membrane.

3.2. Morphologies observation of the porous composite membrane

Figure 4 shows the surface morphology of the porous membrane. Pure KGM were flake-shape, which left some pores created by freeze-drying on it. After compounding with the baking-carbonized functional powder, although the basic characteristics of morphology remained unchanged, the flavor still produced some destruction on the integrity of KGM lamella through creating more pores on surface, and most serious condition happened on the sample prepared by WBTM flavor. In view of preparation, these baking-carbonized functional flavors reshaped the 3D network of KGM as blended with it. When the swelled KGM could not let so many flavor powders to be filled in, macroscopic expansion occurred, which caused the surface layered KGM to be deformed even teared, further create some larger pores on the membrane. Surface pores were not only beneficial for the ice sublimation, but also acted as the channels for smoke flowing.

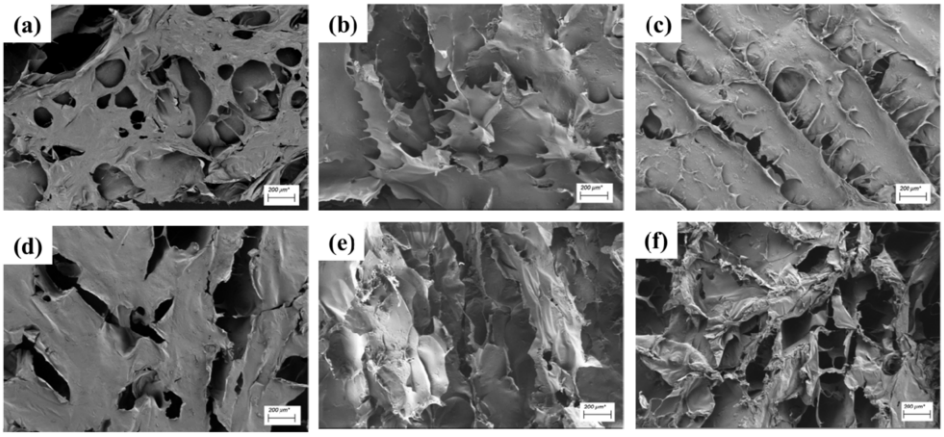

Figure 4. Surface morphologies of the porous composite membranes: (a) pure KGM; (b) ZYFJ(TH)/KGM; (c) ZYFJ/KGM; (d) NTHPEC/KGM; (d) NTHXGXG/KGM; (d) WBTM/KGM.

Figure 5 displays the internal cross-sectional morphology of the porous membrane. The porous composite membrane prepared with ZYFJ, NTHPEC and NTHXGXG still maintained the morphology feature of KGM that the pores left by ice crystals sublimation was orientally arranged. Although there was no directional arrangement of pores on the WBTM contained sample, the lamellar KGM still remains relatively intact and still has a certain pore structure. On the inner section of the ZYFJ (TH) sample, a 3D network of pores constructed by filamentous KGM appeared. It was speculated that the main reason was that the powder agglomerated into in this location and squeezed the space of the KGM lamella, resulting in lamellar KGM.

Further zoom on the right image was to observe that more details about the porosity, there were many salient points on the surface, while the overall smoothness was reduced, especially on the samples of ZYFJ, NTHXGXG was more obvious on the sample. These protrusions were the baking-carbonized functional powders after crushing, which further showed that there was no loss of functional powders during the preparation process of the composite membrane. Therefore, in the film forming stage of KGM, most of the functional powders were wrapped by KGM. In the interior, it would own less impact on the entire membrane to build a three-dimensional network porous

structure through cross-linking. This method of mutual combination was essentially a physical combination. As long as the KGM layer of the porous composite film itself was not damaged, there was no need to worry about the powder loss. When used in a filter, it will not cause the negative sense like coughing, asthma, and others.

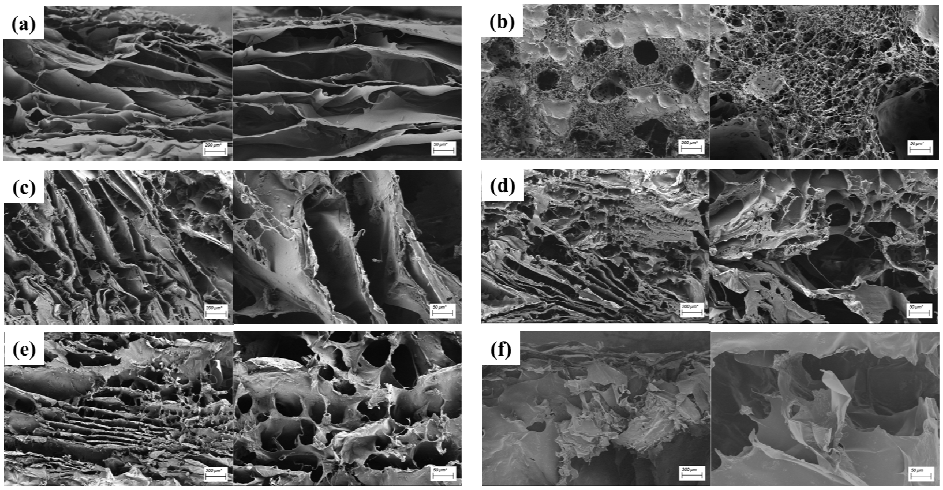

Figure 5. Internal cross-sectional morphologies of the porous composite membranes with different resources: (a) pure KGM; (b) ZYFJ (TH)/KGM; (c) ZYFJ/KGM; (d) NTHPEC/KGM; (d) NTHXGXG/KGM; (d) WBTM/KGM.

3.3. Porosities investigation on the porous composite membrane

Figure 6 is the isothermal N_2 adsorption and desorption curve of the porous composite film after the detection of the fully automatic surface area and porosity analyzer. The sample calculated by the BJH method was in N_2 Pore size distribution during adsorption and pore size distribution during N_2 desorption (from left to right). The isothermal N_2 adsorption and desorption curve of the porous composite film was still type III, which was consistent with the curve characteristics of the KGM porous film and the baking-carbonized particles, and has the characteristic of protruding towards the relative pressure axis. Based on the morphology, it was determined as a macroporous solid, but the interaction between N_2 and pores was weak. The pore size of the porous membrane needs to be further judged by the pore size distribution during desorption.

It could be seen from the pore size distribution at the desorption at right, compared to the nearly 8-40nm mesoporous pore size distribution of the pure KGM porous membrane, the addition of the baked-carbonized powders made the pore size of the porous composite membrane changed into diversity. The porous composite membrane made of ZYFJ (TH) sample owned basically the same pore size distribution range as pure KGM membrane, potentially indicating that the KGM sheet could be ZYFJ (TH) powder was completely wrapped without affecting the inherent three-dimensional network structure. The porous composite membrane made of ZYFJ, NTHXGXG and WBTM, the tip of the pores was not obvious enough, or the mesoporous pores did not exist, if they exist, ZYFJ sample. The pore size of the NTHXGXG sample is concentrated in the range of 4-6nm and 10-5 nm. The pore size of the NTHXGXG

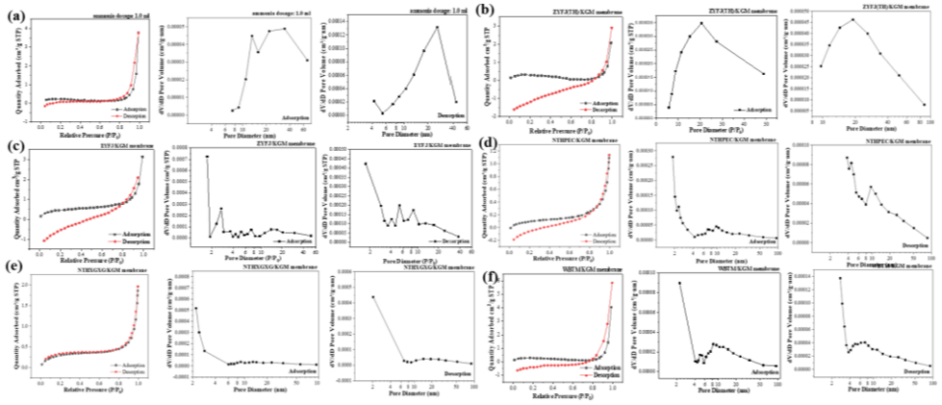

Figure 6. Data obtained by BET test of the porous composite membranes: (a) pure KGM; (b) ZYFJ (TH)/KGM; (c) ZYFJ/KGM; (d) NTHPEC/KGM; (d) NTHXGXG/KGM; (d) WBTM/KGM., left to right: isothermal N_2 adsorption and desorption curve, Pore size distribution of the sample at N_2 adsorption under BJH method, and Pore size distribution at N_2 desorption under BJH method

sample is concentrated in the range of 15-50nm. Take the WBTM porous composite membrane as an example, the pore size distribution shrinks. To the two ranges of 4~10nm and 18-50nm, the specific results need to be judged by the average pore size. The porous composite membrane prepared with NTHPEC has a reduced mesopore pore size, a more concentrated pore size range, and a shrinkage of the pore size distribution to 4-5nm and 8-18nm.

Using the isothermal N2 adsorption and desorption curve for further calculations, more information about the pore structure of the porous composite membrane can be obtained, as summarized in Table 2. It can be seen from the table that after compounding, the specific surface area of porous film is only the exception of WBTM, and the other roasted-carbonized functional powder samples have increased, but the difference between them is relatively small. Combined with the increase in the surface area caused by the powder (bumps) on the KGM sheet under the SEM electron microscope, the specific surface area of the sample is increased, and the total pore volume and the mesopore plus macropore pore volume after the composite of the porous membrane are reduced. There are two reasons. One is that the powdery baked-carbonized functional material does not provide pores, so under the same quality, the proportion of KGM is reduced, and the corresponding pores that can be provided are reduced; the second is from the perspective of the thickness of the composite KGM porous film. It is considered that the thickened sheet layer reduces the pore volume of the three-dimensional porous network structure. What's more noteworthy is that the average pore size of some composite membranes is not consistent with the pore size distribution results. On the samples made of ZYFJ (TH), ZYFJ, NTHXGXG, within the mesoporous pore size range of 2-50 nm, most pores existed with a size smaller than the average size. On the contrary, in WBTM samples, pores larger than the average size are the majority. The pore size and pore number ratio are relatively consistent only with NTHXGXG samples. Considering that the average pore size is calculated based on the assumption of a cylindrical pore structure, under a relatively small pore volume, the larger average pore size indicates that the pore depth of the WBTM composite membrane is relatively low.

Table 2. Mesoporous porosity information of the baking-carbonized functional flavor/KGM porous composite membranes.

Porous membranes	Specific surface area m^2/g	Single point desorption total pore volume of pores cm^3/g	Pore volume of mesopore plus macropore under single point cm^3/g	BJH Desorption average pore diameter nm
Pure KGM	0.6747	0.004160	0.003653	26.7580
ZYFJ(TH)/KGM	1.5215	0.001962	0.001565	28.4009
ZYFJ/KGM	1.9254	0.003588	0.003533	16.5559
NTHPEC/KGM	1.2151	0.001697	0.001697	7.6777
NTHXGXG/KGM	1.4218	0.001862	0.001862	8.5763
WBTM/KGM	1.1368	0.004717	0.004362	24.7735

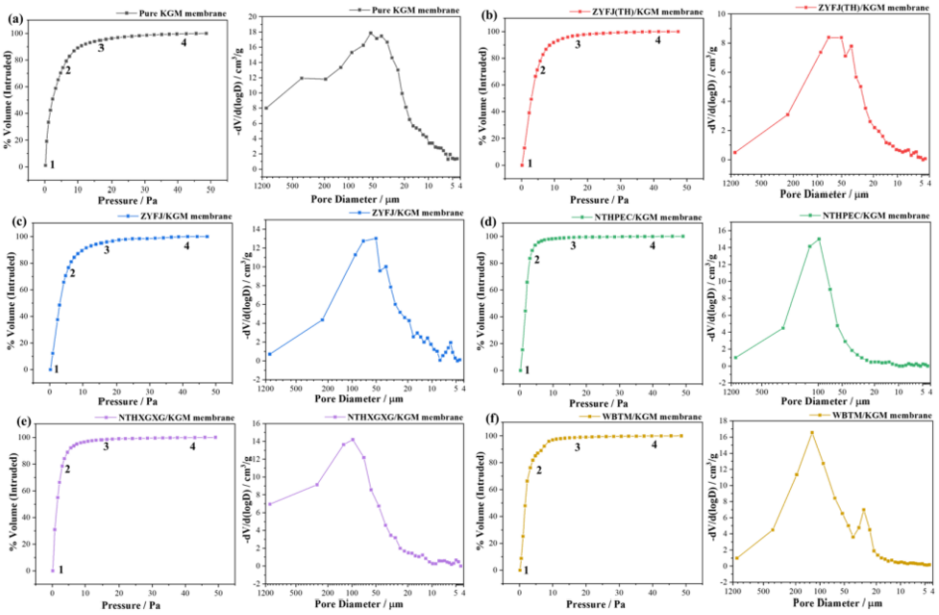

Figure 7. Macroporous structure information of the baking-carbonized functional flavor/KGM porous composite membranes: (a) pure KGM; (b) ZYFJ (TH)/KGM; (c) ZYFJ/KGM; (d) NTHPEC/KGM; (d) NTHXGXG/KGM; (d) WBTM/KGM, left: the mercury intrusion volume and pressurization relationship curve; right: the macropore pore size distribution.

Macroporous pores of the baked-carbonized porous composite membrane were measured by mercury intrusion method, and the results are shown in Figure 7. Left figure was the relationship curve between the volume of mercury intruded and the pressurization. Each point on the curve is the expression in the composite membrane. For the corresponding range of various pore structures, the 1-2-3 segment is macropores. For granular materials, it is mainly the pore volume generated between the voids. For materials with fixed morphology, it represents the inherent macroporous pores, and the higher the steepness, the greater the volume of mercury that can be pressed in, and the material has a larger pore size or a deeper pore depth. In the 3-4 stage, the increase in pressure did not significantly increase the mercury intake, and the energy consumption was mainly manifested in the compression of the material. Comparing the relationship curve between mercury volume and pressurization of pure KGM membrane, the porous composite membrane prepared by ZYFJ (TH), ZYFJ and

WBTM has no significant difference in the 1-2-3 segment, only NTHPEC and NTHXGXG samples are relatively steep, which indicates that the pore size range or depth of the two is higher.

From the right picture obtained from the mercury intrusion test, it can be seen that all samples have macroporous pores over 20μm as a whole, and the pores are distributed in a wide range. The pores are more concentrated in the range of 255-20μm, which is consistent with the SEM observation. The pore size is basically the same. Comparing with each other, it can be seen that the macropore pore size distribution of pure KGM film is relatively wide. After being compounded with the baking-carbonized functional powder, the pore size distribution converges. This change trend is basically consistent with the BET mesoporous pores, which further explains the baking-carbonized functional powder It is wrapped in the sheet layer KGM. In addition, between the porous composite membranes, the ZYFJ sample and the WBTM (Bai Xue tea) sample showed more obvious and concentrated pore distribution in the range of 8.8~5μm and 40~20μm, which may be related to the powder in the depth. The cross-linking and curing stage were related to the reconstruction of the porous structure of the KGM three-dimensional network. NTHPEC and NTHXGXG samples have a narrower macropore pore distribution, combined with their steep mercury intrusion volume-pressurization relationship curve, potentially indicating a deeper pore size or depth.

From the results of the pore size, although the pore size distribution of each sample measured in Figure 7 above is relatively wide, the average pore size is relatively small, which means that most of the porous composite membranes are pores with relatively small pore sizes. From the statistical results in Table 3, the median pore diameter calculated by the median number of pores is larger than the average pore diameter, potentially indicating that in the relatively small pore size, more pores are in the middle position, the pore size is relatively uniform and the difference in the relative size range is small. Compared with the pure KGM porous membrane, when ZYFJ (TH) and ZYFJ are combined, the KGM sheet layer has a good coating effect on the powder, and basically does not affect the three-dimensional network structure of the original KGM membrane. The composite NTHPEC, NTHXGXG and WBTM have a certain Expansion behavior for KGM, that is, the combination of KGM sheets in the membrane becomes worse, and the three-dimensional porous structure is reconstructed. The new macropores can be regarded as damage to the integrity of the porous membrane. This could be verified on the SEM morphology of the WBTM sample.

Table 3. Macroporous porosity information of the baking-carbonized functional flavor/KGM porous composite membranes

Sample naming	Total Porosity %	Intramembrane porosity %	Mean pore diameter μm	Median pore diameter μm
Pure KGM	97.0475	94.0475	46.40	90.77
ZYFJ (TH)/KGM	92.7828	92.7828	49.09	72.27
ZYFJ/KGM	95.6979	95.6979	44.82	69.55
NTHPEC/KGM	94.3914	94.3914	92.25	117.3
NTHXGXG/KGM	96.1605	96.1605	85.63	148.5
WBTM/KGM	95.5625	95.5625	79.94	118.9

3.4. Tensile properties evaluation of the porous composite membrane

Figure 8 showed the tensile mechanical properties of the baking-carbonized functional flavor/KGM porous composite membranes, and (a) depicted the tensile strength, (b)

was the corresponding tensile elasticity modulus. It could be seen from Figure 8(a) that the strengths of all porous composite membrane were significantly lower than that of the pure KGM porous membrane (p at least <0.05), and the average strength of sample prepared by ZYFJ (TH) was relatively higher, while the strength of WBTM samples is the lowest, and there is no significant difference in strength between the remaining roasted-carbonized functional powder samples. The decrease in strength is mainly due to the physical connection between the KGM and the roasting-carbonized functional powder through the form of coating, and no chemical bond can be formed between each other. During stretching, the baked-carbonized functional powder wrapped inside the KGM sheet becomes an obstacle when the porous film is stretched and deformed, which will cause the KGM to crack at a relatively low strain, thereby failing to provide high strength. For porous composite membranes prepared with different baking-carbonization functional powders, the pore volume of the WBTM sample is smaller and the average pore size is larger. The layers are freely combined with each other at a high degree; Considering the total porosity under the macroporous pore structure, relatively small means that the internal KGM is more closely connected to each other, and there are many lamellas that are synchronized and coordinated during deformation. The probability of fracture in turn triggering the fracture of the entire porous mesh is low. The strength of the film is determined by both macroporous pores and mesoporous pores. Macroporous pores will determine the tightness of the bonding of the sheets to each other, and the mesopores can cause the sheet to tear and cause the film to break as a whole. For porous membranes that require high strength, to a certain extent, it is necessary to reduce the porosity (number) of the macropores and reduce the pore size of the mesopores. It can be seen from Figure 8(b) that the decrease in tensile strength will also cause the corresponding decrease in the amount of elastic film. The only thing that does not have a significant difference was the NTHXGXG porous composite film. Compared with different roasting-carbonization functional raw materials, the difference is mainly in the two samples of NTHXGXG and WBTM. The modulus of elasticity is an important parameter to measure the strength and deformation of the material. Too high makes the material have high strength and poor deformability, while too low makes the deformability strong but does not have strength. In this study, except for the low strength and low modulus of the WBTM sample, the strength difference of the

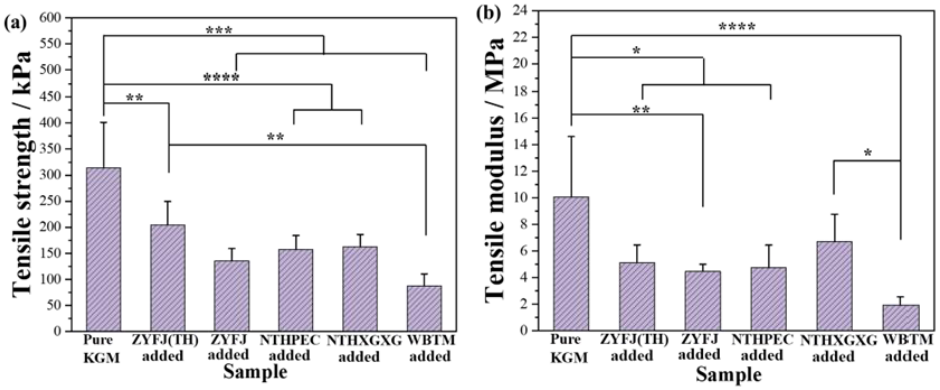

Figure 8. Tensile properties of the baked-carbonized functional flavors/KGM porous composite membrane: (a) tensile strength; (b) tensile elasticity modulus ,the significant difference: *: p<0.05, **: p <0.01, ***: p<0.001, ****: p<0.0001.

other samples is very small. It can be considered that the compressive strength is basically the same, while the elastic modulus of the NTHXGXG sample is higher, which shows that the degree of deformation is low, and it is difficult to apply to the mechanical operation of the subsequent filling into the cigarette filter. The WBTM sample has the risk of deforming and breaking, which will destroy the overall three-dimensional network structure, making the sample develop in the direction of composite particles.

Based on the results and analysis about morphology, mesoporous and macroporous information and tensile mechanical properties, it could be confirmed that the porous membrane that composited with ZYFJ (TH) possessed the best overall performance, which was more suitable to be applied on the filter tip for absorbing the hazardous composition in smoke combining with spreading the special notes of flavor to improve the taste sense.

3.5. Extract ingredients evaluation of the porous composite membranes

Figure 9 is the GC-MS spectrum of the components precipitated in different time periods after the baked-carbonized functional particles/KGM porous composite membrane is subjected to solid-phase microextraction. After the NIST spectral library amtching, pure KGM porous membrane appeared with tridecane, 3, 5-dimethyldodecane, nonanal, tetradecane, carbonic acid, octadecylprop-1-en-2-yl. Main components of ester, nonadecane, 1-hexanol, decanal, 1-anthraceneamine, 13-methyltridecane, 13-methylheptadodecane, propylene glycol, and 1-hexenyl formate, these components have no negative impact on the human body, reflecting the certain biological safety of the KGM film itself. After compounding with 5 kinds of baked-carbonized functional flavors, the detected components were tetrahydrogeranyl formate, 2-heptenal, isopropyl tetradecyl ether, 2-nonenal, Octyl pentafluorooctanoate, octadecyl vinyl ester, ethanol, butanamide, ethyl methacrylate, 2, 4-dichloro-3, 5-

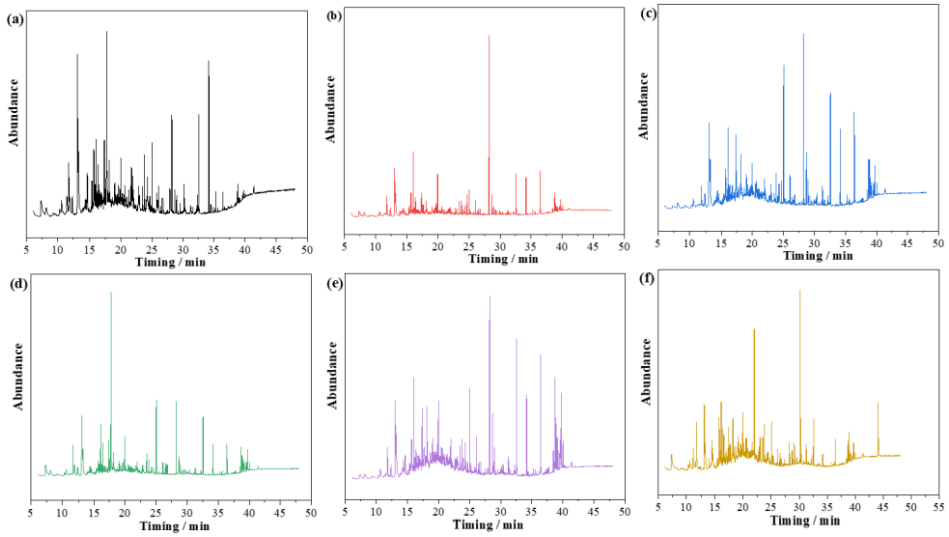

Figure 9. Identification of components by solid-phase microextraction of porous composite membrane: (a) pure KGM; (b) ZYFJ (TH)/KGM; (c) ZYFJ/KGM; (d) NTHPEC/KGM; (d) NTHXGXG/KGM; (d) WBTM/KGM;

dimethylphenol, triacetin, cedarwood, 2, 4-di-tert-butylphenol, m-benzamide and other ingredients. These components have a certain special aroma, and the types and amounts released in different time periods are relatively poor, making the aroma show a comprehensive special aroma. After identification, the baked-carbonized functional particles/KGM porous composite membrane can bring the aroma sensory evaluation of the following Table 4 to cigarette consumers (the test cigarette is cloud smoke) after being installed in the filter.

Combining the morphological characteristics, mesoporous and macroporous pore information, tensile mechanical properties and aroma sensory evaluation of the porous composite membranes, it can be confirmed that the ZYFJ (TH)/KGM composite porous membrane prepared from ebony as raw material has the best comprehensive performance. It can be used for subsequent filling of fragrances or directly used in filters to absorb harmful gases.

3.6. Reduction on hazardous substances as packaged into a commercial cigarette filter

Based on the overall performance of baked-carbonized functional flavors/KGM porous composite membranes, the ZYFJ (TH)/KGM sample as prefer one was packaged into the filter tip of 2 types of commercial cigarette called Yunyan. 7 typical harmful substances of CO, HCN, NNK, NH3, B(a)P, phenol and crotonaldehyde in cigarette smoking was tested and list in Table 4. In TYPE I, the concentrations in μg/piece of most substances emitting in air were decreased as comparing to the control sample, the biggest reduction rate was 26.71% found on phenol, while the concentration of B(a)P seemed to be no obvious change. In TYPE II, the reduction rates on the concentration of were similar to that of TYPE I, 7 hazardous substances were reduced in different degrees, ZYFJ (TH)/KGM porous composite membrane made a significant absorption action on phenol, HCN and crotonaldehyde, especially to the phenol and HCN, both reduction rates were higher than the 13.4% and 1.9% reported by the literature [30]. Besides that, although both CO and B(a)P performed a positive reduction rate, the rate values were too low, which made ZYFJ (TH)/KGM porous composite membrane be considered to fail acting on both substances, the reason needed to be further explored on pore size distribution, and the chemical interaction between porous membrane and hazards [31].

Table 4. Hazardous substances determination after ZYFJ (TH)/KGM porous composite membrane packed in the filter of Yunyan cigarette.

Samples	**Determination Content**						
	CO mg/cigar	**B(a)P** ng/cigar	**NNK** ng/cigar	**Crotonal dehyde** μg/cigar	**HCN** μg/cigar	**NH_3** μg/cigar	**Phenol** μg/cigar
Type I Yunyan (As control)	9.9	6.73	13.36	13.9	102	5.08	14.6
loaded with ZYFJ(TH)/KGM	9.3	6.75	12.09	11.8	81.5	4.62	10.7
Reduction Rate	**6.06%**	**-0.3%**	**9.51%**	**15.11%**	**20.10%**	**9.06%**	**26.71%**
Type II Yunyan (As control)	7.1	4.92	3.53	11.9	79.6	3.33	12.9
loaded with ZYFJ(TH)/KGM	6.9	4.86	3.31	10.2	61.3	3.09	9.9
Reduction Rate	**2.82%**	**1.22%**	**6.23%**	**14.29%**	**22.99%**	**7.21%**	**23.26%**

4. Conclusion

Baking-carbonized functional fragrances prepared in this study are semi-carbonized amorphous carbon with OH-, ≡C-H represented by aldehydes, ketones, hydrocarbons, lactones, alcohols, acids and esters , CH_2, C=O (lipid, aldehyde, ketone, acid), COO-, C-O-C (aldehyde) and C-O-C (ester) and other groups. After being compounded with konjac glucomannan, the functional fragrance is wrapped inside by the water-swelled KGM sheet, forming a three-dimensional network porous structure with KGM as the skeleton, so it has little effect on the pores, and the composite porous film can still maintain 5nm. Mesopores of ~50nm and macropores of 20μm to 255μm, as well as more than 90% intra-membrane porosity and a certain mechanical strength, at the same time, the extracted components show a comprehensive special aroma, which can be used for gas circulation. Provide channels and realize harmful gas adsorption; the extracted components show a comprehensive special aroma, which can achieve the purpose of adding fragrance and moisturizing while adsorbing harmful substances. In contrast, the one prepared with ebony as the raw material has the best comprehensive performance.

Acknowledgement

This work was supported by the Funding of Foundational Project of China Tabacco Yunnan Industrial Co., Ltd. (2020CL04).

References

[1] Kluger R. Ashes to ashes: America's hundred-year cigarette war, the public health, and the unabashed triumph of Philip Morris. New York: Alfred A Knopf, 1996 May: 10-5.

[2] Monrad JK, Howard LR, King JW, Srinivas K, Mauromoustakos A. Subcritical solvent extraction of procyanidins from dried red grape pomace. J Agr Food Chem. 2010 Apr; 58 (7): 4014-21, doi: 10.1021/jf9028283.

[3] Alabadi A, Razzaque S, Yang Y, Chen S, Tan B. Highly porous activated carbon materials from carbonized biomass with high CO_2 capturing capacity. Chem Eng J, 2015 Jun; 281: 606-12. doi: 10.1016/j.cej.2015.06.032.

[4] Torikai K, Uwano Y, Nakamori T, Tarora W, Takahashi H. Study on tobacco components involved in the pyrolytic generation of selected smoke constituents. Food Chem Toxicol. 2005 Apr; 43 (4): 559-68. doi: 10.1016/j.fct.2004.12.011.

[5] Jaszczak E, Polkowska Ż, Narkowicz S, Narkowicz S, Namieśnik J. Cyanides in the environment-analysis-problems and challenges. Environ Sci Pollut Res Int. 2017 Jul; 24 (19): 15929-48. doi: 10.1007/s11356-017-9081-7.

[6] Barbara D, Vivian T, Prue T. Comparison of cytotoxicity of IQOS aerosols to smoke from Marlboro Red and 3R4F reference cigarettes. Toxicol In Vitro. 2019 Dec; 61: 104652. doi: 10.1016/j.tiv.2019.104652.

[7] Wang LY, Liu XY, Chen LS, Liu DS, Yu T, Bai RS, Yan LH, Zhou J. Harmful chemicals of heat not burn product and its induced oxidative stress of macrophages at air-liquid interface: Comparison with ultra-light cigarette. Toxicol Lett. 2020 Oct; 331: 200-07. doi: 10.1016/j.toxlet.2020.06.017.

[8] Han YI, Duan Y, Zhang T, Zhang X, Zhang C. Identification and classification of flavors in 12 tobacco blends using electronic nose. Asian J Chem, 2015 Jan; 27 (2): 396-400. doi: 10.14233/ajchem.2015.16904

[9] Morabito JA, Holman MR, Ding YS, Yan XZ, Chan M, Chafin D, Perez J, Mendez MI, Cardenas RB, Watson C. The use of charcoal in modified cigarette filters for mainstream smoke carbonyl reduction. Regul Toxicol Pharmacol. 2017 Jun; 86: 117-27. doi: 10.1016/j.yrtph.2017.02.019.

[10] Cheng C, Yu X. Research Progress in Chinese Herbal Medicines for Treatment of Sepsis: Pharmacological Action, Phytochemistry, and Pharmacokinetics. Int J Mol Sci. 2021 Oct; 22 (20): 11078. doi: 10.3390/ijms222011078.

[11] McAdam K, Eldridge A, Fearon IM, Liu C, Manson A, Murphy J, Porter A. Influence of cigarette circumference on smoke chemistry, biological activity, and smoking behavior. Regul Toxicol Pharmacol. 2016 Dec; 82: 111-26. doi: 10.1016/j.yrtph.2016.09.010.

[12] Benjamin EJ, Blaha MJ, Chiuve SE, Cushman M, Das SR, Deo R, Ferranti SD, Floyd J, Fornage M, Gillespie C, Isasi CR, Jiménez MC, Jordan LC, Judd SE, Lackland D, Lichtman JH, Lisabeth L, Liu S, Longenecker CT, Mackey RH, Matsushita K, Mozaffarian D, Mussolino ME, Nasir K, Neumar RW, Palaniappan L, Pandey DK, Thiagarajan RR, Reeves MJ, Ritchey M, Rodriguez CJ, Roth GA, Rosamond WD, Sasson C, Towfighi A, Tsao CW, Turner MB, Virani SS, Voeks JH, Willey JZ, Wilkins JT, Wu JH, Alger HM, Wong SS, Muntner P, American HASC and SSS. Heart Disease and Stroke Statistics—2017 Update: A Report From the American Heart Association. Circulation. 2017 Mar; 135 (10): e146-e603. doi: 10.1161/CIR.0000000000000485.

[13] Jia DY, Fang Y, Yao K. Water vapor barrier and mechanical properties of konjac glucomannan–chitosan–soy protein isolate edible films. Food Bioprod Process, 2009 Mar; 87 (1): 7-10. doi: 10.1016/J.FBP.2008.06.002

[14] Chen XH, Pang J, WU CH. Fabrication and Characterization of Antimicrobial Food Packaging Materials Composed of Konjac Glucomannan, Chitosan and Fulvic Acid. Food Sci, 2021 Jul; 42 (7): 232-39. doi: 10.7506/spkx1002-6630-20200417-226.

[15] Liu Z, Lin DH, Lopez-Sanchez P, Yang XB. Characterizations of bacterial cellulose nanofibers reinforced edible films based on konjac glucomannan. Int J Biol Macromol. 2020 Feb; 145: 634-45. doi: 10.1016/j.ijbiomac.2019.12.109.

[16] Wu HJ, Lei YL, Lu JY, Zhu R, Xiao D, Jiao C. Xia R, Zhang ZQ, Shen GH, LiuYT, Li SS, Li ML. Effect of citric acid induced crosslinking on the structure and properties of potato starch/chitosan composite films. Food Hydrocoll, 2019 Dec; 97: 105208. doi: 10.1016/j.foodhyd.2019.105208.

[17] Li B, Xie BJ, Kennedy JF. Studies on the molecular chain morphology of konjac glucomannan. Carbohyd Polym, 2006 Jun; 64 (4): 510-15. doi: 10.1016/j.carbpol.2005.11.001.

[18] Gan L, Shan SM, Hu EL, Yuen CWM, Jiang SXK. Konjac glucomannan/graphene oxide hydrogel with enhanced dyes adsorption capability for methyl blue and methyl orange. Appl Surf Sci, 2015, 357: 866-872. doi: 10.1016/j.apsusc.2015.09.106.

[19] Maleki A, Kjonisen AL, Nystrom B. Characterization of the chemical degradation of Konjac glucomannan during chemical gelation in the presence of different cross-linker agents. Carbohydr Res. 2007 Dec; 342 (18): 2776-92. doi: 10.1016/j.carres.2007.08.021.

[20] Devaraj RD, Reddy CK, Xu BJ. Health-promoting effects of konjac glucomannan and its practical applications: A critical review. Int J Biol Macromol. 2019 Apr; 126: 273-81. doi: 10.1016/j.ijbiomac.2018.12.203.

[21] Chen JH, Wei D, Liu Y, Xiong Y, Peng JJ, Mahmud S, Liu HH. Gold/Konjac glucomannan bionanocomposites for catalytic degradation of mono-azo and di-azo dyes. Inorg Chem Commun, 2020, Otc; 120: 108156. doi: 10.1016/j.inoche.2020.108156.

[22] Xiao M, Tang B, Jiang FT, Wang H, Zheng H, Zhang Y, Xie J, Zhan JB. Formulation Optimization of Konjac Glucomannan-Ethyl Cellulose Composite Film and Its Application in Honey Packaging. Sci Technol Food Indust, 2021, 42 (4): 181-86. doi: 10.13386/j.issn1002-0306.2020050020.

[23] Li ZF, Zheng SQ, Sun HM, Xi R, Sun YQ, Luo DL, Xu W, Jin WP, Shah BR. Structural characterization and antibacterial properties of konjac glucomannan/soluble green tea powder blend films for food packaging. J Food Sci Technol. 2022 Feb; 59 (2): 562-571. doi: 10.1007/s13197-021-05041-4.

[24] Cheng C, Yu X. Research Progress in Chinese Herbal Medicines for Treatment of Sepsis: Pharmacological Action, Phytochemistry, and Pharmacokinetics. Int J Mol Sci. 2021 Oct; 22 (20): 11078. doi: 10.3390/ijms222011078

[25] Huang TH, Zhang J, Tian ZF, Han QY, Liu Q, Xi Yuan, Zhou G. Research Progress on Application of Chinese Herbal Medical Additives to Reduce Harmful Ingredient in Cigarettes. J Henan Agr Sci. 2015 Apr; (4): 4-8. doi: 10.15933/j.cnki.1004-3268.2015.04.002

[26] Huang MH, Chen HB, Chen QH, Tao SG, Chen QG, Yan TT. Study on Nano Hydroxyapatite/Collagen/KGM Porous Bone scaffolds. J Cryst Growth. 2015 Jul; 44 (7): 1961-67. doi: 10.16533/j.cnki.issn1000-985x.2015.07.044.

[27] Mu RJ, Wang L, Du Y, Yuan Y, Ni YS, Wu CH, Pang J. Synthesis of konjac glucomannan-silica hybrid materials with honeycomb structure and its application as activated carbon support for Cu(II) adsorption. Mater Lett. 2018 Sep; 226: 75-78. doi: 10.1016/j.matlet.2018.04.133

[28] Wu CH, Li YZ, Du Y, Wang L, Tong CL, Hu YQ, Pang J, Yan ZM. Preparation and characterization of konjac glucomannan-based bionanocomposite film for active food packaging. Food Hydrocoll. 2019 Apr; 89: 682-90. doi: 10.1016/j.foodhyd.2018.11.001.

[29] Ye SX, Zongo AWS, Shah BR, Li J, Li B. Konjac Glucomannan (KGM), Deacetylated KGM (Da-KGM), and Degraded KGM Derivatives: A Special Focus on Colloidal Nutrition. J Agric Food Chem. 2021 Nov; 69 (44): 12921-32. doi: 10.1021/acs.jafc.1c03647.

[30] Chen JH, Liu Y, Xiong Y, Wei D, Peng JJ, Mahmud S, Li HH. Konjac glucomannan reduced-stabilized silver nanoparticles for mono-azo and di-azo contained wastewater treatment. Inorg Chim Acta. 2022 Jan; 120: 120058. doi: 10.1016/j.ica.2020.120058.

[31] Fan LH, Yi JY, Tong J, Zhou XY, Ge HY, Zou SQ, Wen HG, Nie M. Preparation and characterization of oxidized konjac glucomannan/carboxymethyl chitosan/graphene oxide hydrogel. Int J Biol Macromol. 2016 Oct; 91: 358-67. doi: 10.1016/j.ijbiomac.2016.05.042.